arXiv:1406.1650v2 [quant-ph] 14 Aug 2014

Strong photon antibunching of symmetric and antisymmetric modes in weakly nonlinear photonic molecules

Xun-Wei Xu[1] and Yong Li[1,2,*]

[1]*Beijing Computational Science Research Center, Beijing 100084, China*
[2]*Synergetic Innovation Center of Quantum Information and Quantum Physics, University of Science and Technology of China, Hefei, Anhui 230026, China*

(Dated: August 15, 2014)

We study the photon statistics of symmetric and antisymmetric modes in a photonic molecule consisting of two linearly coupled nonlinear cavity modes. Our calculations show that strong photon antibunching of both symmetric and antisymmetric modes can be obtained even when the nonlinearity in the photonic molecule is weak. The strong antibunching effect results from the destructive interference between different paths for two-photon excitation. Moreover, we find that the optimal frequency detunings for strong photon antibunching in the symmetric and antisymmetric modes are linearly dependent on the coupling strength between the cavity modes in the photonic molecule. This implies that the photonic molecules can be used to generate tunable single-photon sources by tuning the values of the coupling strength between the cavity modes with weak nonlinearity.

PACS numbers: 42.50.Ct, 42.50.Ar, 42.50.Dv

I. INTRODUCTION

Single-photon source is one of the fundamental devices for quantum information processing at single-photon level. In order to create a single-photon source, Imamoglu *et al*. proposed using a high-finesse cavity containing a low density four-level atomic medium [1]. They found that the transmitted photons show strong antibunching. This effect comes from the strong photon-photon interaction: the excitation of a first photon blocks the transport of a second photon for the nonlinear medium in the cavity, called the photon blockade effect. Photon blockade is one of the mechanisms for creating strong antibunching photons. In 2005 photon blockade was observed in an optical cavity with one trapped atom [2, 3]. Subsequently, a sequence of experimental groups observed the strong antibunching behaviors in different systems: a quantum dot in a photonic crystal [4], circuit cavity quantum electrodynamics (QED) systems [5–7].

Recently, Liew and Savona found a new mechanism in a photonic molecule consisting of two linearly coupled nonlinear cavity modes that can give rise to strong photon antibunching even with nonlinearities much smaller than the decay rates of the cavity modes [8]. The physical explanation is that the strong photon-photon correlation was attributed to the destructive quantum interference effect in the nonlinear photonic molecule [9, 10]. Based on this mechanism, many different systems are proposed to achieve photon blockade, such as bimodal optical cavity with a quantum dot [11, 12], coupled optomechanical systems [13, 14], a double quantum well embedded in a micropillar optical cavity [15], and coupled single-mode cavities with second- or third-order nonlinearity [16–18].

The statistic properties of photons in the photonic molecules have already been studied in Refs. [8–18], focusing on the statistic properties of photons for modes located in one of the cavities. However, as the coupling between the photonic cavities reaches the strong coupling regime, the photonic eigenmodes are the symmetric and antisymmetric modes spanning the whole system [19–28]. Nonclassical photon correlations for the symmetric and antisymmetric modes in two-mode optomechanics have already been studied theoretically, and it was shown that the nonlinear interactions can be significantly enhanced in the coupled optomechanics [27, 28].

In this paper, we will investigate the photon statistics of the symmetric and antisymmetric modes, instead of local modes, in a photonic molecule consisting of two linearly coupled nonlinear cavities, and show that the photons of both the symmetric and antisymmetric modes can exhibit strong antibunching effect even with weak nonlinearity in the photonic molecule. Most importantly, different from the result given in Refs. [8, 9], we find that the optimal frequency detunings for strong photon antibunching in the symmetric and antisymmetric modes are linearly dependent on the coupling strength between the cavity modes. So we can generate tunable single-photon sources by the symmetric and antisymmetric modes in the photonic molecules with weak nonlinearity.

The paper is organized as follows: In Sec. II, we will show the Hamiltonian and the dynamic equation of the photonic molecule system. In Sec. III, the statistic properties of the photons of the symmetric and antisymmetric modes in the photonic molecule are investigated via the second-order correlation functions by numerical calculations. In Sec. IV, the optimal conditions for strong antibunching effect are obtained analytically. Finally, we draw our conclusions in Sec. V.

II. PHYSICAL MODEL

Photonic molecule consists of two nonlinear cavity modes with coupling strength J. Taking the coupled microtoroids for an example, as shown in Fig. 1, the coupling strength between the cavity modes in the two microtoroids depends exponentially upon the air gap [19, 20]. The distance and hence the

*Electronic address: liyong@csrc.ac.cn

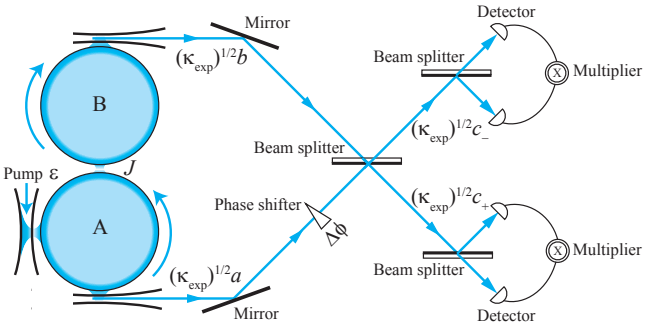

FIG. 1: (Color online) Schematic diagram of setup for the detection of photon antibunching effects of symmetric and antisymmetric modes in a photonic molecule consisting of two tunnel-coupled nonlinear microtoroids. $\kappa_{\rm exp}$ is the loss rate for detection.

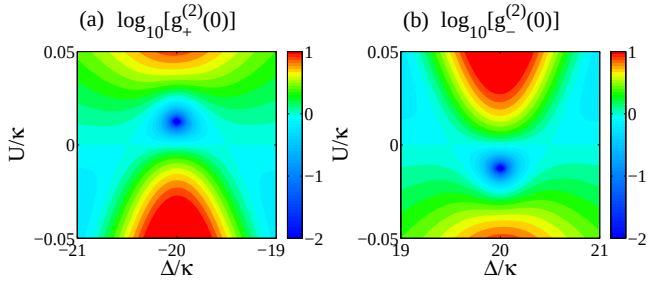

FIG. 2: (Color online) Logarithmic plot (of base 10) of the equal-time second-order correlation functions $g_{\pm}^{(2)}(0)$ as functions of the detuning Δ and the nonlinear interaction strength U/κ for the coupling strength $J = 20\kappa$ and Rabi frequency $\varepsilon = 0.01\kappa$.

coupling between the cavity modes in the microtoroids can be controlled precisely [21–25]. The Hamiltonian for the compound system in a frame rotating at the frequency of the driving field ω_d reads [8] ($\hbar = 1$):

$$\begin{aligned} H &= \Delta_a a^\dagger a + \Delta_b b^\dagger b - J\left(a^\dagger b + b^\dagger a\right) \\ &\quad + U a^\dagger a^\dagger a a + U b^\dagger b^\dagger b b + \varepsilon\left(a^\dagger + a\right), \end{aligned} \tag{1}$$

where a (b) is a bosonic operator for cavity mode A (B) with frequency ω_a (ω_b); U is the Kerr nonlinear interaction strength in each cavity. ε is the Rabi frequency of the external driving field and has been assumed to be real; $\Delta_a = \omega_a - \omega_d$ ($\Delta_b = \omega_b - \omega_d$) is the frequency detuning between the cavity mode and the driving field. For simplicity, we assume that the frequencies of the two cavity modes are the same, i.e. $\Delta_a = \Delta_b = \Delta$, then the cavity modes in the photonic molecule can be combined to form the symmetric and antisymmetric modes by $c_\pm = (a \pm b)/\sqrt{2}$, and the Hamiltonian is transformed into

$$\begin{aligned} H &= (\Delta - J)\, c_+^\dagger c_+ + (\Delta + J)\, c_-^\dagger c_- \\ &\quad + \frac{U}{2}\left(c_+^\dagger c_+^\dagger c_+ c_+ + c_-^\dagger c_-^\dagger c_- c_-\right) \\ &\quad + \frac{U}{2}\left(c_-^\dagger c_-^\dagger c_+ c_+ + c_+^\dagger c_+^\dagger c_- c_- + 4 c_+^\dagger c_+ c_-^\dagger c_-\right) \\ &\quad + \frac{\varepsilon}{\sqrt{2}}\left(c_+^\dagger + c_-^\dagger\right) + \frac{\varepsilon}{\sqrt{2}}\left(c_+ + c_-\right). \end{aligned} \tag{2}$$

There are only nonlinear couplings between the symmetric and antisymmetric modes [29].

The dynamics of the system can be described by the master equation for the density matrix ρ,

$$\begin{aligned} \frac{\partial \rho}{\partial t} &= -i\left[H, \rho\right] \\ &\quad + \frac{\kappa_a + \kappa_b}{4}\left(2 c_+ \rho c_+^\dagger - c_+^\dagger c_+ \rho - \rho c_+^\dagger c_+\right) \\ &\quad + \frac{\kappa_a + \kappa_b}{4}\left(2 c_- \rho c_-^\dagger - c_-^\dagger c_- \rho - \rho c_-^\dagger c_-\right) \\ &\quad + \frac{\kappa_a - \kappa_b}{4}\left(2 c_+ \rho c_-^\dagger - c_+^\dagger c_- \rho - \rho c_+^\dagger c_-\right) \\ &\quad + \frac{\kappa_a - \kappa_b}{4}\left(2 c_- \rho c_+^\dagger - c_-^\dagger c_+ \rho - \rho c_-^\dagger c_+\right), \end{aligned} \tag{3}$$

where κ_a (κ_b) is the dissipation rate which includes the loss rate $\kappa_{\rm exp}$ (i.e. wave guide coupling) for detection. The equilibrium mean thermal photon numbers in cavity modes at optical frequencies have been neglected. Without loss of generality, we assume that the dissipation rates of the cavity modes are equal, i.e. $\kappa_a = \kappa_b = \kappa$, then the coupling terms induced by the dissipation in the master equation (last two terms) vanish. The master equation can be solved by expanding the density matrix over a Fock basis [8, 13, 30].

In this paper, we will focus on the statistic properties of photons for the symmetric and antisymmetric modes in the photonic molecule, which are described by the second-order correlation functions as

$$g_\pm^{(2)}(\tau) = \frac{\left\langle c_\pm^\dagger(0)\, c_\pm^\dagger(\tau)\, c_\pm(\tau)\, c_\pm(0)\right\rangle}{\left\langle c_\pm^\dagger(0)\, c_\pm(0)\right\rangle^2} \tag{4}$$

in the steady state, where τ is the time delay between different detectors. In experiments, the statistic properties of photons for the symmetric and antisymmetric modes can be obtained by combining the two output fields from cavity modes A and B through a 50/50 beam splitter, and detecting the statistic properties of photons for the symmetric and antisymmetric modes individually by the Hanbury Brown-Twiss experiment [31], as shown in Fig. 1. In theory, we can solve the master equation numerically to get the density matrix ρ within a truncated Fock space, then the second-order correlation functions for the symmetric and antisymmetric modes are obtained.

III. NUMERICAL RESULTS

In this section, the second-order correlation functions $g_\pm^{(2)}(\tau)$ will be plotted as functions of various parameters by solving the master equation numerically within a truncated Fock space. We assume that the external driving field are weak, with Rabi frequency $\varepsilon = 0.01\kappa$. Such a weak driving condition is a necessary condition for photon blockade [7] and small truncated Fock space (five photons are retained in the following numerical calculations). For convenience, we

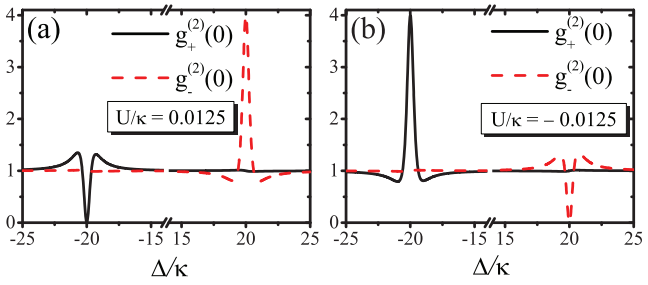

FIG. 3: (Color online) The equal-time second-order correlation functions $g_{\pm}^{(2)}(0)$ plotted as functions of the detuning Δ/κ for nonlinear interaction strength (a) $U/\kappa = 0.0125$ and (b) $U/\kappa = -0.0125$. The parameters are $J = 20\kappa$ and $\varepsilon = 0.01\kappa$.

normalize all the parameters to the dissipation rate of the cavity modes κ.

In order to find the optimal conditions for strong antibunching numerically, we show the logarithmic plot of the equal-time second-order correlation functions $g_{\pm}^{(2)}(0)$ as functions of the detuning Δ/κ and the nonlinear interaction strength U/κ for the coupling strength $J = 20\kappa$ in Fig. 2. We note that there is a dip regime for $g_{+}^{(2)}(0) \ll 1$ around the point $\Delta = -20\kappa$, $U = 0.0125\kappa$, corresponding to strong antibunching in the symmetric mode. Similarly, there is a dip regime for $g_{-}^{(2)}(0) \ll 1$ around the point $\Delta = 20\kappa$, $U = -0.0125\kappa$, corresponding to strong antibunching in the antisymmetric mode.

In Fig. 3, we show the equal-time second-order correlation functions $g_{\pm}^{(2)}(0)$ as functions of the detuning Δ/κ. For the nonlinear interaction strength $U/\kappa = 0.0125$ and coupling strength $J/\kappa = 20$, $g_{+}^{(2)}(0) \ll 1$ at $\Delta = -J = -20\kappa$, while $g_{-}^{(2)}(0) > 1$ at $\Delta = J = 20\kappa$. On the contrary, for the nonlinear interaction strength $U/\kappa = -0.0125$, $g_{-}^{(2)}(0) \ll 1$ around the point $\Delta = J = 20\kappa$, while $g_{+}^{(2)}(0) > 1$ around the point $\Delta = -J = -20\kappa$. These indicate that, the photons for the symmetric (antisymetric) mode exhibit strong antibunching effect as the detuning $\Delta = -J$ ($\Delta = J$) with weak nonlinear interaction strength $U/\kappa = 0.0125$ ($U/\kappa = -0.0125$).

The equal-time second-order correlation functions $g_{\pm}^{(2)}(0)$ as functions of nonlinear interaction strength U normalized to κ^2/J is shown in Fig. 4. This plot show that the photons for the symmetric mode exhibit antibunching as nonlinear interaction strength $0 < U/(\kappa^2/J) < 1/2$ with $\Delta = -J$ and reach optimal strong antibunching at $U/(\kappa^2/J) = 1/4$; the photons for the antisymmetric mode exhibit antibunching as nonlinear interaction strength $-1/2 < U/(\kappa^2/J) < 0$ with the detuning $\Delta = J$ and reach optimal strong antibunching at $U/(\kappa^2/J) = -1/4$.

As the statistic properties of photons for the symmetric and antisymmetric modes are similar to each other, let us focus on the case of the symmetric mode in the following. A two-dimensional plot of the equal-time second-order correlation function $g_{+}^{(2)}(0)$ as a function of nonlinear interaction strength U/κ and coupling strength J/κ for $\Delta = -J$ is shown

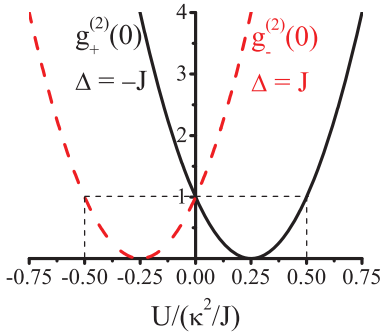

FIG. 4: (Color online) The equal-time second-order correlation functions $g_{\pm}^{(2)}(0)$ as functions of nonlinear interaction strength U normalized to κ^2/J with Rabi frequency $\varepsilon = 0.01\kappa$. (Black solid line) $g_{+}^{(2)}(0)$ for $\Delta = -J = -20\kappa$; (Red dash line) $g_{-}^{(2)}(0)$ for $\Delta = J = 20\kappa$.

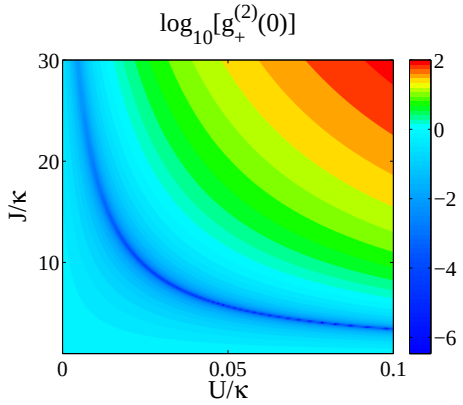

FIG. 5: (Color online) Logarithmic plot (of base 10) of the equal-time second-order correlation function $g_{+}^{(2)}(0)$ as a function of nonlinear interaction strength U/κ and coupling strength J/κ for $\Delta = -J$ and $\varepsilon = 0.01\kappa$.

in Fig. 5. With increasing J/κ, the value of U/κ for getting the strong antibunching (dark blue regime in the figure) descends gradually. That is to say, the requirement of the nonlinear interaction strength U for obtaining strong photon antibunching in the symmetric mode can be controlled by tuning the value of the coupling strength J in the photonic molecule.

The equal-time second-order correlation function $g_{+}^{(2)}(0)$ as a function of the detuning Δ/κ for different coupling strengths J/κ are shown in Fig. 6, where $U/\kappa = \kappa/(4J)$. With the increase of J, the optimal detuning for strong antibunching in the symmetric mode shifts as $\Delta = -J$. As a consequence, we can shift the optimal value of the detuning for strong antibunching in the symmetric mode by tuning the coupling strength J in the photonic molecule. This is significantly different from the result given in Refs. [8, 9], where the optimal detuning is fixed at $\Delta/\kappa = \pm 1/(2\sqrt{3})$ in the strong coupling condition $J \gg \kappa$ [9]. As the coupling between the microtoroids can be controlled precisely in the experiments [21, 23, 25], the symmetric and antisymmetric modes in photonic molecules with weak nonlinearity can be

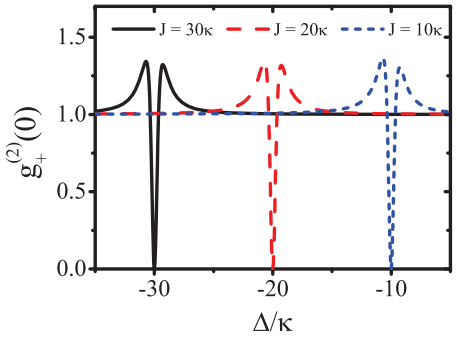

FIG. 6: (Color online) The equal-time second-order correlation function $g_+^{(2)}(0)$ as a function of the detuning Δ/κ for different values of the coupling strength J with nonlinear interaction strength $U/\kappa = \kappa/(4J)$ and Rabi frequency $\varepsilon = 0.01\kappa$: (black solid line) $J = 30\kappa$; (red dash line) $J = 20\kappa$; (blue short dash line) $J = 10\kappa$.

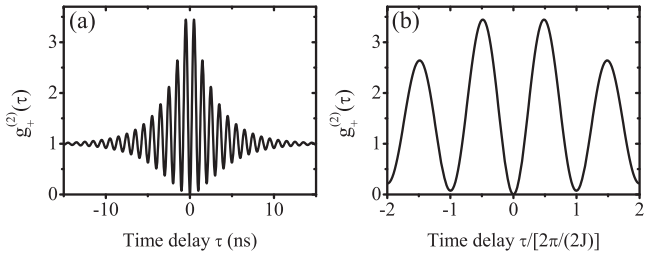

FIG. 7: (a) The second-order correlation functions $g_+^{(2)}(\tau)$ as a function of the time delay τ. (b) $g_+^{(2)}(\tau)$ as a function of the normalized time delay $\tau/[2\pi/(2J)]$. The parameters are $\Delta = -5\kappa$, $J = 5\kappa$, $U = 0.05\kappa$, $\varepsilon = 0.01\kappa$ and $\kappa = 2\pi \times 100$ MHz.

used to generate tunable single-photon sources.

Now, let us do some discussions about the feasibility of the strong photon antibunching effect for weak nonlinearity with some realistic parameters. For the experiment in Ref. [21], the resonance frequency for cavity mode is about 200 THz, the Q-factor is 4×10^7 for empty cavity and the coupling strength between the two cavity modes ranges from 5 MHz to nearly 5 GHz. The Q-factor for the microtoroid made from silica doped with Kerr medium should become lower, and $Q = 3 \times 10^6$ for the microtoroid made from silica doped with gain-medium was obtained in Ref. [23].

After considering the parameters in the experiments [21, 23], we take the parameters $\kappa = 2\pi \times 100$ MHz and $J = 5\kappa$ for numerical calculations, and the second-order correlation function $g_+^{(2)}(\tau)$ is plotted as a function of the time delay τ in Fig. 7. Similar to the reports given in Refs. [8, 9, 13], $g_+^{(2)}(\tau)$ shows an oscillation behavior as the delay time going on with the period $2\pi/(2J)$ [as shown in Fig. 7(b)]. The magnitude of the oscillation decreases as the increase of τ and almost approaches unity as $\tau \geq 10$ ns [as shown in Fig. 7(a)], which is about the lifetime of the photons in the cavities. This oscillation behavior comes from the Rabi oscillation between the photon states and we will explain this in detail in the end of next section.

IV. OPTIMAL CONDITIONS

In order to understand the origin of the above strong antibunching obtained numerically, we will derive the optimal conditions analytically following the method given in Ref. [9]. In the weak driving condition $\varepsilon \ll \kappa$, we expand the wave function on a Fock-state basis of symmetric and antisymmetric modes truncated to the two-photon manifold with the ansatz:

$$\begin{aligned}|\psi\rangle &= C_{00}|0,0\rangle + C_{10}|1,0\rangle + C_{01}|0,1\rangle \\ &\quad + C_{20}|2,0\rangle + C_{11}|1,1\rangle + C_{02}|0,2\rangle . \end{aligned} \quad (5)$$

Here, $|n_+, n_-\rangle$ represents the Fock state with n_+ photons in the symmetric mode and n_- photons in the antisymmetric mode. Substituting the wave function [Eq. (5)] and Hamiltonian [Eq. (2)] into the Schrodinger's equation, we get the dynamic equations for the coefficients $C_{n_+n_-}$:

$$\begin{aligned} i\frac{\partial}{\partial t}C_{00} &= \frac{\varepsilon}{\sqrt{2}}C_{10} + \frac{\varepsilon}{\sqrt{2}}C_{01}, \\ i\frac{\partial}{\partial t}C_{10} &= \left(\Delta - J - i\frac{\kappa}{2}\right)C_{10} + \frac{\varepsilon}{\sqrt{2}}(C_{00} + C_{11}) + \varepsilon C_{20}, \\ i\frac{\partial}{\partial t}C_{01} &= \left(\Delta + J - i\frac{\kappa}{2}\right)C_{01} + \frac{\varepsilon}{\sqrt{2}}(C_{00} + C_{11}) + \varepsilon C_{02}, \\ i\frac{\partial}{\partial t}C_{20} &= \left[U + 2\left(\Delta - J - i\frac{\kappa}{2}\right)\right]C_{20} + \varepsilon C_{10} + UC_{02}, \\ i\frac{\partial}{\partial t}C_{02} &= \left[U + 2\left(\Delta + J - i\frac{\kappa}{2}\right)\right]C_{02} + \varepsilon C_{01} + UC_{20}, \\ i\frac{\partial}{\partial t}C_{11} &= \frac{\varepsilon}{\sqrt{2}}(C_{01} + C_{10}) + (2\Delta - i\kappa + 2U)C_{11}. \end{aligned} \quad (6)$$

Under the weak driving condition $\varepsilon \ll \kappa$, we have $|C_{00}| \gg |C_{10}|, |C_{01}| \gg |C_{20}|, |C_{11}|, |C_{02}|$, and the equations for the coefficients of one-photon states,

$$\left(\Delta - J - i\frac{\kappa}{2}\right)C_{10} = -\frac{\varepsilon}{\sqrt{2}}C_{00}, \quad (7)$$

$$\left(\Delta + J - i\frac{\kappa}{2}\right)C_{01} = -\frac{\varepsilon}{\sqrt{2}}C_{00}, \quad (8)$$

and for the coefficients of two-photon states,

$$0 = \left[U + 2\left(\Delta - J - i\frac{\kappa}{2}\right)\right]C_{20} + UC_{02} + \varepsilon C_{10}, \quad (9)$$

$$0 = \left[U + 2\left(\Delta + J - i\frac{\kappa}{2}\right)\right]C_{02} + UC_{20} + \varepsilon C_{01}, \quad (10)$$

$$0 = (2\Delta - i\kappa + 2U)C_{11} + \frac{\varepsilon}{\sqrt{2}}(C_{01} + C_{10}). \quad (11)$$

From Eqs. (7)-(8), the relation between C_{10} and C_{01} reads

$$\frac{C_{10}}{C_{01}} = \frac{\Delta + J - i\frac{\kappa}{2}}{\Delta - J - i\frac{\kappa}{2}} = \frac{1}{\eta}. \quad (12)$$

Substituting this relation into Eqs. (10)-(11), we get

$$0 = \left[U + 2\left(\Delta + J - i\frac{\kappa}{2}\right)\right]C_{02} + UC_{20} + \varepsilon\eta C_{10}, \quad (13)$$

$$0 = (2\Delta - i\kappa + 2U)C_{11} + \frac{\varepsilon}{\sqrt{2}}\frac{2\Delta - i\kappa}{\Delta - J - i\frac{\kappa}{2}}C_{01}. \quad (14)$$

The conditions for $g_+^{(2)}(0) \ll 1$ are derived from Eqs. (9) and (13) by setting $C_{20} = 0$, so we get

$$0 = UC_{02} + \varepsilon C_{10}, \quad (15)$$

$$0 = \left[U + 2\left(\Delta + J - i\frac{\kappa}{2}\right)\right] C_{02} + \varepsilon\eta C_{10}. \quad (16)$$

The condition for that C_{10} and C_{02} have non-trival solutions is that the determinant of the coefficient matrices of Eqs. (15)-(16) equals to zero, then we get the equation for optimal photon antibunching as

$$\frac{\kappa^2}{4} - JU - (\Delta + J)^2 + i(\Delta + J)\kappa = 0. \quad (17)$$

For the imagine part to be zero, we have

$$\Delta_{\rm opt} = -J, \quad (18)$$

and for the real part equal to be zero, we get

$$\frac{U_{\rm opt}}{\kappa} = \frac{\kappa}{4J}. \quad (19)$$

Eqs. (18)-(19) are the optimal conditions for $g_+^{(2)}(0) \ll 1$ in Fig. 2-5.

Similarly, we can get the optimal conditions for $g_-^{(2)}(0) \ll 1$ from Eqs. (9)-(11) by using the relation between C_{10} and C_{01} [Eq. (12)] and setting $C_{02} = 0$, then we get

$$0 = \left[U + 2\left(\Delta - J - i\frac{\kappa}{2}\right)\right] C_{20} + \frac{\varepsilon}{\eta} C_{01}, \quad (20)$$

$$0 = UC_{20} + \varepsilon C_{01}. \quad (21)$$

To make sure C_{01} and C_{20} have non-trival solutions, we have

$$\frac{\kappa^2}{4} + JU - (\Delta - J)^2 + i(\Delta - J)\kappa = 0. \quad (22)$$

Then, the optimal conditions for $g_-^{(2)}(0) \ll 1$ are given by

$$\Delta_{\rm opt} = J, \quad (23)$$

$$\frac{U_{\rm opt}}{\kappa} = -\frac{\kappa}{4J}. \quad (24)$$

In Fig. 8, we show the energy-level diagram and the transition paths. There are two paths for two-photon excitation in the symmetric mode: (i) directly exciting two photons in the symmetric mode (red lines with arrows), i.e. $|0,0\rangle \overset{\varepsilon/\sqrt{2}}{\rightarrow} |1,0\rangle \overset{\varepsilon}{\rightarrow} |2,0\rangle$; (ii) exciting two photons in the antisymmetric mode (cyan lines with arrows), then coupling to the the symmetric mode via the nonlinear interaction (green line with arrows): i.e. $|0,0\rangle \overset{\varepsilon/\sqrt{2}}{\rightarrow} |0,1\rangle \overset{\varepsilon}{\rightarrow} |0,2\rangle \overset{U}{\rightarrow} |2,0\rangle$. These two paths lead to the destructive quantum interference that is responsible for the strong antibunching in the symmetric mode. Moreover, the fact that the optimal nonlinear interaction strength is inversely proportional to the coupling strength J [$U_{\rm opt}/\kappa = \kappa/(4J)$] can be understood as follows: For $\Delta_{\rm opt} = -J$, with the increase of the coupling strength between the cavity modes J, the non-resonant transition $|0,0\rangle \overset{\varepsilon/\sqrt{2}}{\rightarrow} |1,0\rangle \overset{\varepsilon}{\rightarrow} |2,0\rangle$ will be suppressed, while the resonant transition $|0,0\rangle \overset{\varepsilon/\sqrt{2}}{\rightarrow} |0,1\rangle \overset{\varepsilon}{\rightarrow} |0,2\rangle$ will be enhanced, so the nonlinear interaction strength U needed for destructive quantum interference becomes smaller. Similar origin leads to the strong antibunching effect in the antisymmetric mode.

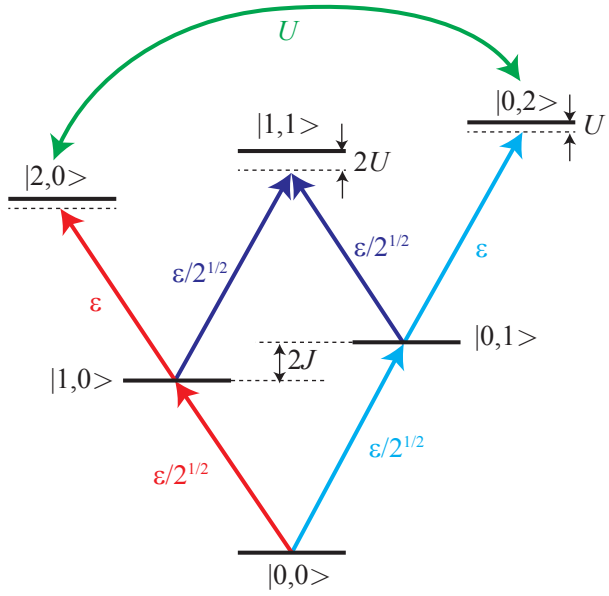

FIG. 8: (Color online) Energy-level diagram showing the zero-, one- and two-photon states (horizontal black short lines) and the transition paths leading to the quantum interference responsible for the strong antibunching (color lines with arrows). $|n_+, n_-\rangle$ represents the Fock state with n_+ photons in the symmetric mode and n_- photons in the antisymmetric mode.

Finally, let us give an explanation for the oscillation behavior of $g_+^{(2)}(\tau)$ (as shown in Fig. 7) via the energy-level diagram (Fig. 8). In the short time approximation $t \ll 2\pi/\kappa \ll 2\pi/\varepsilon$, we can treat the transitions $|0,0\rangle \overset{\varepsilon/\sqrt{2}}{\rightarrow} |1,0\rangle$ and $|0,0\rangle \overset{\varepsilon/\sqrt{2}}{\rightarrow} |0,1\rangle$ as two individual Rabi models with the system in the vacuum state initially. For $\Delta = -J$, the driving field is resonant with the transitions $|0,0\rangle \rightarrow |0,1\rangle$ while the detuning between driving field and the transitions $|0,0\rangle \rightarrow |1,0\rangle$ is $2J$, so we have $|C_{01}|^2 \simeq \left[1 - \cos(\sqrt{2}\epsilon t)\right]/2$ and $|C_{10}|^2 \simeq [1 - \cos(2Jt)]\varepsilon^2/(4J^2)$. The time oscillation of $g_+^{(2)}(\tau)$ with period $2\pi/(2J)$ comes from the Rabi oscillation between $|0,0\rangle$ and $|1,0\rangle$.

V. CONCLUSIONS

In summary, we have studied the photon statistics of the symmetric and antisymmetric modes in the photonic molecule consisting of two linearly coupled nonlinear cavity modes. Due to the destructive quantum interference effect between the different paths for two-photon excitation, the photons of

both the symmetric and antisymmetric modes can exhibit strong antibunching effect even with weak nonlinear interaction in the photonic molecule. By analytical method, we show that the optimal frequency detunings for strong photon antibunching in the symmetric and antisymmetric modes are linearly dependent on the coupling strength between the nonlinear cavity modes in the photonic molecule. Thus we can control the statistic properties of the photons by tuning the coupling strength between the nonlinear cavity modes in the photonic molecule. Our results may have important applications in generating tunable single-photon sources.

Acknowledgement

We thank Y. L. Liu, L. Ge, X. Xiao, Q. Zheng and Y. Yao for fruitful discussions. This work is supported by the Postdoctoral Science Foundation of China (under Grant No. 2014M550019), the NSFC (under Grant No. 11174027), and the National 973 program (under Grant No. 2012CB922104 and No. 2014CB921402).

[1] A. Imamo$\bar{g}$lu, H. Schmidt, G. Woods, and M. Deutsch, Phys. Rev. Lett. **79**, 1467 (1997).
[2] K. M. Birnbaum, A. Boca, R. Miller, A. D. Boozer, T. E. Northup, and H. J. Kimble, Nature (London) **436**, 87 (2005).
[3] B. Dayan, A. S. Parkins, T. Aoki, E. P. Ostby, K. J. Vahala, and H. J. Kimble, Science **319**, 1062 (2008).
[4] A. Faraon, I. Fushman, D. Englund, N. Stoltz, P. Petroff, and J. Vučković, Nature Phys. **4**, 859 (2008).
[5] C. Lang, D. Bozyigit, C. Eichler, L. Steffen, J. M. Fink, A. A. Abdumalikov, Jr., M. Baur, S. Filipp, M. P. da Silva, A. Blais, and A. Wallraff, Phys. Rev. Lett. **106**, 243601 (2011).
[6] A. J. Hoffman, S. J. Srinivasan, S. Schmidt, L. Spietz, J. Aumentado, H. E. Türeci, and A. A. Houck, Phys. Rev. Lett. **107**, 053602 (2011).
[7] Y. X. Liu, X. W. Xu, A. Miranowicz, and F. Nori, Phys. Rev. A **89**, 043818 (2014).
[8] T. C. H. Liew and V. Savona, Phys. Rev. Lett. **104**, 183601 (2010).
[9] M. Bamba, A. Imamoğlu, I. Carusotto, and C. Ciuti, Phys. Rev. A **83**, 021802(R) (2011).
[10] I. Carusotto and C. Ciuti, Rev. Mod. Phys. **85**, 299 (2013).
[11] A. Majumdar, M. Bajcsy, A. Rundquist, and J. Vučković, Phys. Rev. Lett. **108** 183601 (2012).
[12] W. Zhang, Z. Y. Yu, Y. M. Liu, and Y. W. Peng, Phys. Rev. A **89**, 043832 (2014).
[13] X. W. Xu and Y. J. Li, J. Opt. B: At. Mol. Opt. Phys. **46**, 035502 (2013).
[14] V. Savona, arXiv:1302.5937 (2013).
[15] O. Kyriienko, I. A. Shelykh, T. C. H. Liew, arXiv:1403.7441v1 (2014).
[16] S. Ferretti, V. Savona, and D. Gerace, New J. Phys. **15**, 025012 (2013).
[17] H. Flayac and V. Savona, Phys. Rev. A **88**, 033836 (2013).
[18] D. Gerace and V. Savona, Phys. Rev. A **89**, 031803(R) (2014).
[19] V. S. Ilchenko, M. L. Gorodetsky, and S. P. Vyatchanin, Opt. Commun. **107**, 41 (1994).
[20] A. Nakagawa, S. Ishii, and T. Baba, Appl. Phys. Lett. **86**, 041112 (2005).
[21] I. S. Grudinin, H. Lee, O. Painter, and K. J. Vahala, Phys. Rev. Lett. **104**, 083901 (2010).
[22] B. Peng, S. K. Ozdemir, J. Zhu, and L. Yang, Opt. Lett. **37**, 3435 (2012).
[23] B. Peng, S. K. Ozdemir, F. C. Lei, F. Monifi, M. Gianfreda, G. L. Long, S. H. Fan, F. Nori, C. M. Bender, and L. Yang, Nature Phys. **10**, 394 (2014).
[24] L. Chang, X. S. Jiang, S. Y. Hua, C. Yang, J. M. Wen, L. Jiang, G. Y. Li, G. Z. Wang, and M. Xiao, Nature photon. **8**, 524 (2014).
[25] B. Peng, S. K. Ozdemir, W. J. Chen, F. Nori, and L. Yang, arXiv:1404.5941 (2014).
[26] M. Ludwig, A. H. Safavi-Naeini, O. Painter, and F. Marquardt, Phys. Rev. Lett. **109**, 063601 (2012).
[27] K. Stannigel, P. Komar, S. J. M. Habraken, S. D. Bennett, M. D. Lukin, P. Zoller, and P. Rabl, Phys. Rev. Lett. **109**, 013603 (2012).
[28] P. Komar, S. D. Bennett, K. Stannigel, S. J. M. Habraken, P. Rabl, P. Zoller, and M. D. Lukin, Phys. Rev. A **87**, 013839 (2013).
[29] Y. F. Xiao, S. K. Ozdemir, V. Gaddam, C. H. Dong, N. Imoto, and L. Yang, Opt. Express **16**, 21462 (2008).
[30] A. Verger, C. Ciuti, and I. Carusotto, Phys. Rev. B **73**, 193306 (2006).
[31] H.-A. Bachor and T. C. Ralph, *A Guide to Experiments in Quantum Optics* (Wiley VCH, Weinheim, 2004).